Fidelity Witnesses for Fermionic Quantum Simulations

M. Gluza,[1] M. Kliesch,[2,3] J. Eisert,[1] and L. Aolita[4,5,6]
[1]*Dahlem Center for Complex Quantum Systems, Freie Universität Berlin, Germany*
[2]*Institute of Theoretical Physics and Astrophysics, University of Gdańsk, Poland*
[3]*Institute for Theoretical Physics, Heinrich Heine University Düsseldorf, 40225 Düsseldorf, Germany*
[4]*Instituto de Física, Universidade Federal do Rio de Janeiro, P.O. Box 68528, Rio de Janeiro, Rio de Janeiro 21941-972, Brazil*
[5]*International Institute of Physics, Federal University of Rio Grande do Norte, 59070-405 Natal, Brazil*
[6]*ICTP South American Institute for Fundamental Research, Instituto de Física Teórica, UNESP-Universidade Estadual Paulista R. Dr. Bento T. Ferraz 271, Bl. II, São Paulo 01140-070, São Paulo, Brazil*

(Received 26 May 2017; published 11 May 2018)

The experimental interest and developments in quantum spin-1/2 chains has increased uninterruptedly over the past decade. In many instances, the target quantum simulation belongs to the broader class of noninteracting fermionic models, constituting an important benchmark. In spite of this class being analytically efficiently tractable, no direct certification tool has yet been reported for it. In fact, in experiments, certification has almost exclusively relied on notions of quantum state tomography scaling very unfavorably with the system size. Here, we develop experimentally friendly fidelity witnesses for all pure fermionic Gaussian target states. Their expectation value yields a tight lower bound to the fidelity and can be measured efficiently. We derive witnesses in full generality in the Majorana-fermion representation and apply them to experimentally relevant spin-1/2 chains. Among others, we show how to efficiently certify strongly out-of-equilibrium dynamics in critical Ising chains. At the heart of the measurement scheme is a variant of importance sampling specially tailored to overlaps between covariance matrices. The method is shown to be robust against finite experimental-state infidelities.

DOI: 10.1103/PhysRevLett.120.190501

Quantum simulators are specific-purpose quantum devices that are able to efficiently simulate phenomena of interest thought to be not directly accessible otherwise [1]. Already at scales of tens of particles they have the potential to outperform today's most powerful supercomputers and help us explain unclear physical effects, as well as give boosts in crucial technological areas [2]. In addition, they constitute an intermediate milestone towards the ultimate goal of realizing large-scale universal quantum computers. This has fueled impressive experimental advances in multiple quantum technologies [3–9]. A type of quantum many-body systems to which experimental simulations have devoted considerable efforts over the past decade is given by one-dimensional lattices of interacting spin-1/2 particles, or spin-1/2 chains, for short. In particular, even though they fall into the regime of efficient classical simulatability, the well-known transverse-field (TF) Ising and XY models have become important basic test beds for the most advanced experimental simulations, e.g., with ion-trap [10–13], superconducting-circuit [14], Rydberg-atom [15], and circuit quantum electrodynamics [16] platforms, including digitalized simulations [12,14,16].

At least two facts justify the significant interest in these specific models. The first one is that they display a vast physical richness: For instance, the TF Ising model—which is, actually, a subclass of the TF XY model—features a quantum phase transition [17–20] as well as topologically and spectrally interesting effects [21–25], and is relevant for quantum speed-ups in certain optimization problems [26]. The second one is that, for nearest-neighbor interactions, they can be analytically solved, e.g., by mapping them into systems of free, i.e., noninteracting, fermions [17]. This allows for in-depth theoretical studies of their dynamics [27–32]. From a broader perspective, these models belong to a more general class of exactly solvable systems known as noninteracting quantum systems, also referred to as fermionic linear optics [33–39]. This class is the fermionic counterpart of the Gaussian formalism for bosons [40,41], which plays a major role in quantum information and quantum optics. It includes, e.g., tight-binding models important in condensed-matter physics, certain interacting bosonic chains that can be fermionized [42–44], and spin-1/2 systems in two-dimensional lattices, such as the celebrated Kitaev's honeycomb model [37], which exhibits non-Abelian excitations.

Unfortunately, the exact analytical solution of a model does not imply that one can efficiently *certify* the correctness of an uncharacterized experimental simulation of it. Furthermore, even if the computational complexity of the target simulation is low, the number of measurements required for its certification can be exponentially high in the lattice size without the adequate certification method. This is the case, e.g., for full state tomography (FST). Characterization tools not relying on FST exist [45–54], each

one efficient on a different subclass of simulations. However, none of these can efficiently handle fermionic linear optics. In fact, almost all [10–12,14,16] the abovementioned experiments relied on FST. The simulation of Ref. [13], in contrast, was certified with matrix-product state tomography [48]. This is a powerful method that covers a broad class of chains but tolerates little long-range entanglement, so that nontrivial evolutions are in practice tractable only over short times [13,48]. Indeed, generic spin chains out of the equilibrium [55], or even very natural, static free-fermionic states [56,57], involve large amounts of entanglement along the lattice. Today, a major roadblock for further experimental progress in spin-chain simulations (and in many-body quantum technologies in general) is their certification.

Here, we develop efficient *fidelity witnesses* for all pure fermionic Gaussian target states. These are experimentally friendly observables whose expectation value (on an arbitrary experimental state) yields a tight lower bound to the fidelity with the target. Hence, they allow for *unconditional* certification, i.e., without any *a priori* knowledge of the experimental setup or imperfections. We derive the witnesses in full generality in the Majorana-fermion representation, and then apply them to experimentally relevant spin-1/2 chains as examples. Among others, we show how to efficiently certify any *sudden quench* (i.e., strongly out-of-equilibrium dynamics) in a critical TF Ising chain with nearest-neighbor interactions. The measurement scheme relies on *importance sampling* tailored to overlaps between covariance matrices, which is potentially interesting on its own. As a result, the number of measurements required for the certification only has a modest scaling with the lattice size, i.e., a small *sample complexity*, for which we present upper bounds. Moreover, the method is robust against finite experimental-state infidelities, in the sense of there always existing a closed ball of valid states that are correctly accepted by the certification test. Finally, we provide also a totally general construction, not restricted to fermions or Gaussian states, of (possibly nonefficient) fidelity witnesses for arbitrary pure target states, which may also be useful in other scenarios.

Preliminaries.—Consider a system of L spinless fermionic atoms, from now on referred to as fermionic modes. By $f_j^\dagger$ and f_j we denote the creation and annihilation operators, respectively, where $j = 1, 2, \ldots, L$. They satisfy the canonical anticommutation relations $\{f_j, f_k^\dagger\} = f_j f_k^\dagger + f_k^\dagger f_j = \delta_{j,k}$ and $\{f_j, f_k\} = \{f_j^\dagger, f_k^\dagger\} = 0$, with $\delta_{j,k}$ the Kronecker symbol. Let us next introduce the self-adjoint Majorana mode operators,

$$m_{2j-1} := f_j + f_j^\dagger, \qquad m_{2j} := -i(f_j - f_j^\dagger), \tag{1}$$

with anticommutation relations $\{m_j, m_k\} = 2\delta_{j,k}$. We say that the fermionic system is free, Gaussian, or linear optical [33–39] if it is governed by a quadratic Hamiltonian,

$$H = \frac{i}{4}\sum_{j,k=1}^{2L} A_{j,k} m_j m_k, \tag{2}$$

where $\boldsymbol{A} = -\boldsymbol{A}^\top \in \mathbb{R}^{2L\times 2L}$ is called the coupling matrix.

The term "free" or "noninteracting" stems from the fact that H is unitarily equivalent to a Hamiltonian of L fermions not featuring any off-diagonal couplings. In the bosonic realm, this is the defining property of Gaussian systems [40,41], which justifies the term Gaussian. In turn, what is linear about fermionic linear optics is the time evolution of the mode operators in the Heisenberg picture,

$$m_j(t) := U^\dagger(t) m_j U(t) = \sum_{k=1}^{2L} Q_{j,k}(t) m_k, \tag{3}$$

where $U(t) := e^{-iHt}$, for $t \in \mathbb{R}$, is a fermionic Gaussian unitary and $\boldsymbol{Q}(t) := e^{t\boldsymbol{A}} \in \mathbb{SO}(2L)$ its representation in mode space [58]; see Appendix A of Supplemental Material for a simple derivation [59].

Finally, it is useful to introduce, for any state ϱ (Gaussian or not), the real antisymmetric covariance matrix $\boldsymbol{M}(\varrho)$ with elements

$$M_{j,k}(\varrho) := \frac{i}{2}\mathrm{tr}([m_j, m_k]\varrho). \tag{4}$$

This matrix contains the expectation values of the single-mode densities $\langle n_j\rangle := \langle f_j^\dagger f_j\rangle$ as well as the two-mode currents $\langle f_j^\dagger f_k + \mathrm{H.c.}\rangle$ and pairing terms $\langle f_j^\dagger f_k^\dagger + \mathrm{H.c.}\rangle$.

Fidelity witnesses.—We consider throughout a (known) pure target state ϱ_t and an arbitrary, unknown experimental preparation ϱ_p. Their closeness is measured by their *fidelity*,

$$F := F(\varrho_t, \varrho_p) := \mathrm{tr}[(\sqrt{\varrho_t}\varrho_p^\dagger\sqrt{\varrho_t})^{1/2}]^2 = \mathrm{tr}[\varrho_t\varrho_p], \tag{5}$$

where the last equality holds because ϱ_t is pure. With this, the pivotal notion of our work can be defined as follows.

Definition 1 [Fidelity witnesses].—An observable $\mathcal{W}$ is a fidelity witness for ϱ_t if, for $F_{\mathcal{W}}(\varrho_p) := \mathrm{tr}[\mathcal{W}\varrho_p]$, it holds that (i) $F_{\mathcal{W}}(\varrho_p) = 1$ if, and only if, $\varrho_p = \varrho_t$, and (ii) $F_{\mathcal{W}}(\varrho_p) \le F$ for all states ϱ_p.

The term "witness" refers to the property that, for any fixed threshold F_T, finding $F_{\mathcal{W}}(\varrho_p) \ge F_T$ witnesses that $F \ge F_T$, but if $F_{\mathcal{W}}(\varrho_p) < F_T$ is found, then nothing can be said about F (see Fig. 1). This is the least information about ϱ_p needed to certify its fidelity with ϱ_t. The situation is reminiscent of entanglement witnesses [62], which detect *some* entangled states and discard all nonentangled ones. The difference is that fidelity witnesses explicitly realize the extremality-based intuition of "corralling valid states against the boundary." Specific witnesses have been built for ground states of local Hamiltonians [48,54,63] and

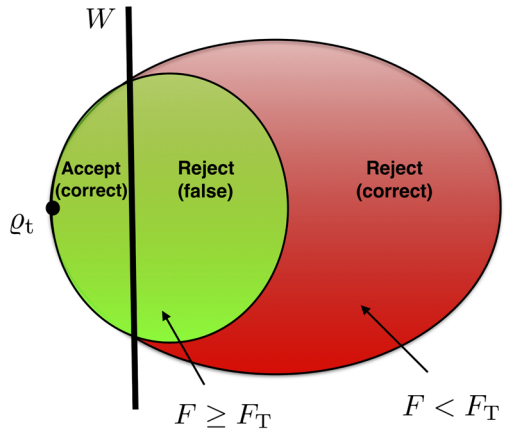

FIG. 1. Geometrical representation of a fidelity witness. A pure target state ϱ_t lies at the boundary of state space. For any fixed fidelity threshold F_T, the valid experimental states are defined by $F \geq F_T$ (green). The states with $F < F_T$ are invalid (red). A fidelity witness $\mathcal{W}$ defines a hyperplane (straight line), to the left of which only valid states are found and to the right of which both valid as well as invalid ones are found. The certification test consists of accepting all states on the left and rejecting all those on the right. Hence, a significant subset of valid states is sacrificed, as in weak-membership problems. However, in return, the experimental estimation is considerably more efficient than in schemes attempting to separate the valid from the invalid states (strong-membership problems).

Gaussian as well as non-Gaussian output states of bosonic linear-optical circuits [52]. In Appendix B of Supplemental Material we present (possibly nonefficient) fidelity witnesses of arbitrary target states with no assumption other than being pure [59]. A special case of such generic construction is the following (efficient) witnesses for the free-fermionic setting.

Any L-mode pure fermionic Gaussian target state ϱ_t can be written as

$$\varrho_t := |\psi_t\rangle\langle\psi_t| \quad \text{with} \quad |\psi_t\rangle := U|\boldsymbol{\omega}\rangle, \tag{6}$$

for a fermionic Gaussian unitary U, as defined below Eq. (3), where $\boldsymbol{\omega} := (\omega_1, \ldots, \omega_L)$ is an L-bit string. The ket $|\boldsymbol{\omega}\rangle$ represents the Fock-basis state vector with $\omega_j \in \{0, 1\}$ excitations in mode j, i.e., $n_j|\boldsymbol{\omega}\rangle = \omega_j|\boldsymbol{\omega}\rangle$, for $j = 1, \ldots, L$, and $n_j := f_j^\dagger f_j$. It is also convenient to introduce $n^{(\boldsymbol{\omega})} := \sum_{j=1}^{L} [(1-\omega_j)n_j + \omega_j(\mathbb{1} - n_j)]$, the total fermion-number operator in the locally flipped basis in which $\boldsymbol{\omega}$ is the null string, i.e., $n^{(\boldsymbol{\omega})}|\boldsymbol{\omega}\rangle = 0$. In other words, $|\psi_t\rangle$ represents the so-called Fermi-sea state and the eigenstates of $n^{(\boldsymbol{\omega})}$ its excitations. In Appendix B [59], we show that the observable

$$\mathcal{W} = U(\mathbb{1} - n^{(\boldsymbol{\omega})})U^\dagger \tag{7}$$

is a fidelity witness for ϱ_t. Expression (7) is the fermionic analogue of the bosonic Gausssian-state witnesses of Ref. [52], with a crucial difference: While for bosons only the Fock-basis state vector $|\mathbf{0}\rangle$ is Gaussian, for fermions all 2^L Fock-basis vectors $|\boldsymbol{\nu}\rangle$ are Gaussian as they satisfy Wick's theorem [36]. In fact, for mixed states, all single-mode states are Gaussian, in sharp contrast to the bosonic case.

Measurement scheme.—Taking the expectation value of Eq. (7) with state ϱ_p yields (see Appendix C [59])

$$F_{\mathcal{W}}(\varrho_p) = 1 + \frac{1}{4}\mathrm{tr}[(\boldsymbol{M}(\varrho_p) - \boldsymbol{M}(\varrho_t))^\top \boldsymbol{M}(\varrho_t)], \tag{8}$$

where $\boldsymbol{M}(\varrho_p)$ and $\boldsymbol{M}(\varrho_t)$ are the covariance matrices of ϱ_t and ϱ_p, respectively. This expression holds also for bosonic Gaussian witnesses [52] and turns out to be very useful for the measurement of $F_{\mathcal{W}}(\varrho_p)$. We call $\Omega := \{(j,k) : M_{j,k}(\varrho_t) \neq 0, \quad \text{for } 1 \leq j < k \leq 2L\}$ the set of nonzero entries of $\boldsymbol{M}(\varrho_t)$. Then Eqs. (4) and (8) imply that if one measures on ϱ_p all $|\Omega| \leq 2L^2 + L$ observables $im_j m_k$ with indices in Ω, then one can estimate $F_{\mathcal{W}}(\varrho_p)$. However, this is not the most efficient procedure (see Appendixes D and E [59]).

A more efficient approach is to exploit importance sampling techniques, where a subset of the $|\Omega|$ observables is randomly selected for measurement according to its importance for $\mathcal{W}$. These techniques have been applied in Hilbert space to the estimation of state overlaps, where they yield efficient schemes only for a specific type of target states [49,50]. Here we apply them in mode space to efficiently estimate overlaps between fully general covariance matrices. The starting point is to identify a random variable X and an importance distribution $P := \{P_\mu\}_\mu$, with X taking the value X_μ with probability P_μ, such that $\mathrm{tr}[\boldsymbol{M}(\varrho_p)^\top \boldsymbol{M}(\varrho_t)]$ is expressed as the mean value of X, i.e.,

$$\mathbb{E}[X] = \sum_\mu P_\mu X_\mu = \mathrm{tr}[\boldsymbol{M}(\varrho_p)^\top \boldsymbol{M}(\varrho_t)]. \tag{9}$$

Then, if one can experimentally sample X from P, $\mathbb{E}[X]$ can be approximated by the finite-sample average $\mathcal{X}^* := \sum_{m=1}^{\mathcal{N}} X_{\mu(m)}/\mathcal{N}$, where $X_{\mu(m)}$ is the value of X at the mth experimental run and $\mathcal{N}$ is the total sample size (number of runs). Next, we present a choice of X and P particularly suited to estimate $F_{\mathcal{W}}(\varrho_p)$.

To this end, let us first define $\hat{m}_{j,k}^{(\beta)}$ as the projector onto the eigenstate of the observable $im_j m_k$ with eigenvalue $\beta = \pm 1$, for $(j,k) \in \Omega$. Then, identifying μ with the triple (β, j, k) and using the short-hand notation

$$|\boldsymbol{M}(\varrho_t)| := \sum_{(j,k)\in\Omega} |M_{j,k}(\varrho_t)| \leq 2L^2, \tag{10}$$

we choose

$$X_{\beta,j,k} \coloneqq 2|\boldsymbol{M}(\varrho_t)|\beta \mathrm{sgn}[M_{j,k}(\varrho_t)] \tag{11}$$

and

$$P_{\beta,j,k} \coloneqq \frac{\mathrm{tr}[\hat{m}^{(\beta)}_{j,k}\varrho_p]|M_{j,k}(\varrho_t)|}{|\boldsymbol{M}(\varrho_t)|}. \tag{12}$$

This choice satisfies Eq. (9), as explicitly shown in Appendix D [59]. In the experiment, in turn, for each run one chooses (j,k) according to $P_{j,k} \coloneqq |M_{j,k}(\varrho_t)|/|\boldsymbol{M}(\varrho_t)|$ and measures im_jm_k on ϱ_p, which outputs β with probability $P_{\beta|j,k} \coloneqq \mathrm{tr}[\hat{m}^{(\beta)}_{j,k}\varrho_p]$. Substituting the obtained (j,k) and β in Eq. (11), one samples $X_{\beta,j,k}$ with probability $P_{\beta,j,k}$, as desired. As for the experimental accessibility of the observables, for the relevant case of spin-1/2 chains, each im_jm_k corresponds to a product of Pauli matrices, as discussed below.

This single-shot importance sampling approach does not necessarily yield a good estimate of each individual entry of $\boldsymbol{M}(\varrho_p)$, as unlikely observables according to $P_{j,k}$ are measured seldomly. The method is specially tailored to directly obtain $F_{\mathcal{W}}(\varrho_p)$. In fact, the resulting estimate $\mathcal{X}^*$ yields an excellent approximation of $\mathrm{tr}[\boldsymbol{M}(\varrho_p)^\top \boldsymbol{M}(\varrho_t)]$ (in a formal sense given by Theorem 2 below), with which the right-hand side of Eq. (8) can be immediately evaluated. This gives our final finite-sample estimate $F^*_{\mathcal{W}}(\varrho_p)$ of $F_{\mathcal{W}}(\varrho_p)$.

Sample complexity.—Let $\mathcal{N}_{\epsilon,\delta}(\mathcal{W})$ be the minimum number (over all estimation strategies) of single measurements required to estimate $F_{\mathcal{W}}(\varrho_p)$, up to maximal statistical error ϵ and with maximal failure probability δ, i.e., such that

$$\mathbb{P}(|F_{\mathcal{W}}(\varrho_p) - F^*_{\mathcal{W}}(\varrho_p)| \leq \epsilon) \geq 1-\delta, \tag{13}$$

for all ϱ_p. Then the scaling of $\mathcal{N}_{\epsilon,\delta}(\mathcal{W})$ with L is called the sample complexity [51,52,64] of estimating $F_{\mathcal{W}}(\varrho_p)$. In Appendix D we compute the number of single measurements required with the measurement scheme described above [59], which sets the following upper bound on $\mathcal{N}_{\epsilon,\delta}(\mathcal{W})$.

Theorem 2 [Sample complexity of $F_{\mathcal{W}}$].—Let $\epsilon > 0$, $\delta \in (0,1)$, ϱ_t given by Eq. (6), and $\mathcal{W}$ by Eq. (7). Then,

$$\mathcal{N}_{\epsilon,\delta}(\mathcal{W}) \leq \left\lceil \frac{\ln(2/\delta)|\boldsymbol{M}(\varrho_t)|^2}{2\epsilon^2} \right\rceil. \tag{14}$$

Equation (10) implies that the right-hand side of Eq. (14) is never larger than $\lceil 2\ln(2/\delta)L^4/\epsilon^2 \rceil$. The scaling is thus polynomial in L for all ϱ_t, which means that the scheme is efficient in the lattice size. Furthermore, for the physically relevant case of ϱ_t being the unique ground state of a local gapped Hamiltonian, the correlations $\mathrm{tr}([m_j,m_k]\varrho_t)$ decay exponentially with $|j-k|$ [65]. Then, $|\boldsymbol{M}(\varrho_t)| \sim L\log(L)$, which leads to $\mathcal{N}_{\epsilon,\delta}(\mathcal{W}) \leq O(L^2\log^2(L))$.

Finally, in Appendix E, we study also a measurement scheme without importance sampling (where all $|\Omega|$ observables are measured) but exploiting the fact that all commuting observables with indices in Ω can be measured simultaneously in each measurement run [59]. This gives the bound $\mathcal{N}_{\epsilon,\delta}(\mathcal{W}) \leq O(2\ln(2|\Omega|/\delta)L^4/\epsilon^2)$, which, since $|\Omega| \leq 2L^2 + L$, scales logarithmically worse in L than in Eq. (14). We suspect that the bound in Eq. (14) is close to being tight.

Spin-1/2 chains.—We denote a local spin operator acting at site k by $\sigma^\alpha_k = \mathbb{1}_2^{\otimes(k-1)} \otimes \sigma^\alpha \otimes \mathbb{1}_2^{\otimes(L-k)}$, where σ^α for $\alpha = x,y,z$ are the Pauli matrices and $\mathbb{1}_2$ is the single-qubit identity. Via the Jordan-Wigner transformation [66,67]

$$m_{2k-1} = \left(\prod_{j<k}\sigma^z_j\right)\sigma^x_k, \qquad m_{2k} = \left(\prod_{j<k}\sigma^z_j\right)\sigma^y_k, \tag{15}$$

the Hamiltonian in Eq. (2) is equivalent [17] to the experimentally relevant [10–16] spin-1/2 Hamiltonian

$$H_{\mathrm{spin}} = -\sum_{k=1}^{L-1}\left(J^x_k\sigma^x_j\sigma^x_{k+1} + J^y_k\sigma^y_k\sigma^y_{k+1}\right) - \sum_{k=1}^{L}B_k\sigma^z_k, \tag{16}$$

where $J^x_k, J^y_k \in \mathbb{R}$ and $B_k \in \mathbb{R}$ are, respectively, constant coupling and transverse-field strengths. Since these chains are equivalent to free-fermionic systems for all parameter regimes, certifying simulations of, e.g., both adiabatic ground state preparations and sudden quenches amounts to certifying pure fermionic Gaussian states, as described above. Finally, note that Eqs. (15) map each im_jm_k to a product of Pauli matrices, as anticipated in the measurement scheme above.

Sudden quenches in critical Ising chains.—The 1D nearest-neighbor TF Ising Hamiltonian is given by Eq. (16) with $J^x_k = J$, $J^y = 0$, and $B_k = B$, for all $k = 1,\ldots,L$, where $J, B > 0$. In a typical quench, the initial ground state $|\psi(0)\rangle \coloneqq |\uparrow\rangle^{\otimes L}$ at a noncritical regime $J = 0 < B$, where $|\uparrow\rangle$ is an eigenvector of σ^z, is evolved under the critical regime $J = B$, so as to generate a strong out-of-equilibrium evolution. These quenches are particularly challenging to certify [13,48] because the time-evolved state vector $|\psi(t)\rangle$ rapidly acquires large amounts of entanglement. Let us consider the simulation of such a quench by a digital quantum simulator, which approximates the continuous-time evolution with a Trotter-Suzuki pulse sequence $U(t) = e^{-it(H_B+H_J)} \approx U_T \coloneqq (e^{-i\Delta t H_B}e^{-i\Delta t H_J})^T$, where $t = T\Delta t$ and H_B and H_J are the Ising Hamiltonians for $J = 0$ and $B = 0$, respectively. The target covariance matrix is then $\boldsymbol{M}(\varrho_t) = \boldsymbol{Q}(t)\boldsymbol{M}(|\uparrow\rangle\langle\uparrow|^{\otimes L})\boldsymbol{Q}(t)^\top$, where $\boldsymbol{Q}(t) = e^{t\boldsymbol{A}(J,B)}$, with $\boldsymbol{A}(J,B)$ the coupling matrix of $H_B + H_J$, is the mode representation of the target time propagator $U(t)$ and

$$\boldsymbol{M}(|\uparrow\rangle\langle\uparrow|^{\otimes L}) \coloneqq \oplus_{j=1}^{L} \begin{pmatrix} 0 & -1 \\ 1 & 0 \end{pmatrix}. \tag{17}$$

In turn, the preparation's covariance matrix is given by $\boldsymbol{M}(\varrho_p) = \boldsymbol{Q}_T \boldsymbol{M}(|\uparrow\rangle\langle\uparrow|^{\otimes L}) \boldsymbol{Q}_T^{\top}$, where $\boldsymbol{Q}_T = (e^{\Delta t \boldsymbol{A}(J)} e^{\Delta t \boldsymbol{A}(B)})^T$, with $\boldsymbol{A}(J)$ $[\boldsymbol{A}(B)]$ the coupling matrix of H_B $[H_J]$, corresponds to the discrete-time experimental evolution U_T. See Fig. 2 for numerical results and Appendix A of Supplemental Material [59] for details.

Discussion.—We have shown how to certify experimental states of dimension 2^{2L} with at most $O(L^4)$ measurements, with no assumption whatsoever on the experimental imperfections, for all pure fermionic Gaussian target states. Moreover, for targets given by ground states of gapped free-fermionic Hamiltonians, the number of experimental repetitions reduces to $O(L^2 \log^2(L))$. In addition, in Appendix F we prove that there always exists a closed ball of valid states that are correctly accepted by the certification test, so that the test is robust against finite experimental deviations [59].

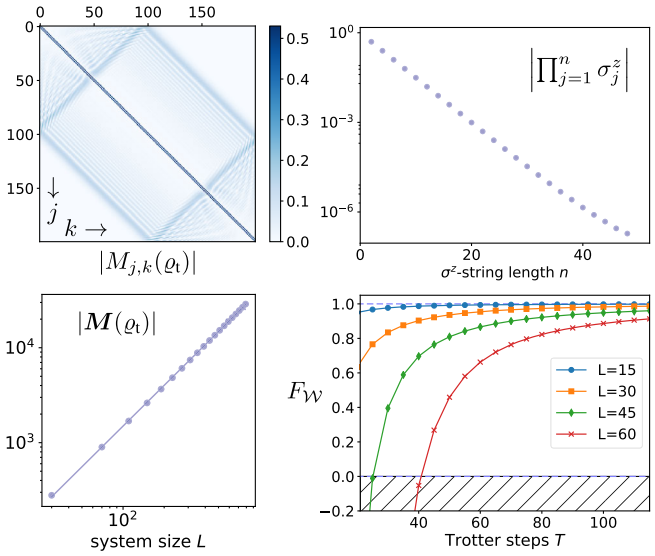

FIG. 2. Certification of a sudden quench in a critical spin-1/2 chain. The target state vector is given by $|\uparrow\rangle^{\otimes L}$ evolved, under the TF Ising Hamiltonian with $J = 1 = B$, up to time $t = L/8$, where L is the number of spins. Top left-hand panel: Absolute values of the $4L^2$ entries of the target covariance matrix for $L = 100$. The plot shows the correlation wave front propagating parallel to the diagonal. At $t = L/8$, the wave front has explored half the lattice size, in the sense that long-range correlations between spins of lattice distance $L/2$ have developed. Top right-hand panel: An extensive amount of Pauli matrix products (only one of which is shown) have exponentially small expectation values on the target state. This renders importance sampling in Hilbert space [49,50] inapplicable. Importance sampling in mode space, in contrast, is efficient for estimating overlaps between arbitrary covariance matrices (see text). Bottom left-hand panel: $|\boldsymbol{M}(\varrho_t)|$ as a function of L, with a power fit yielding the scaling $|\boldsymbol{M}(\varrho_t)| \approx 2.11 \times L^{1.42}$, so that the sample complexity is bounded by $\mathcal{N}_{\epsilon,\delta}(\mathcal{W}) \lesssim O(L^{2.84})$. Bottom right-hand panel: Expectation value of the fidelity witness, as a function of L, on a preparation of the continuous-time evolved state by a digital quantum simulator with T Trotter-Suzuki pulses. As L increases, T needs to increase to keep a value of the fidelity lower bound constant.

Our results are directly relevant to recent experiments with spin chains [7,10–16,68] as well as potential implementations of Kitaev's honeycomb model [69,70]. For instance, concerning the certification of sudden quenches as in Ref. [13], our technique is not limited by the generated long-range entanglement and therefore applies to long-time dynamics, for nearest-neighbor interactions. In turn, as for certifying adiabatic passages of the type of Ref. [15], again for nearest-neighbor interactions, our technique may be useful even for evolutions stopping close to criticality. Additionally, in real-life digital simulations [12,14,16], apart from the Trotterization errors, also heating and noise will of course be present. The fidelity witnesses offer an excellent tool for experimentally quantifying, in an inexpensive way, the detrimental effects of such imperfections on the simulation's performance.

Free-fermionic models are classically tractable, but the importance of their quantum simulations comes from the fact that they constitute a test bed for experimental many-body quantum technologies, with certified simulations of classically intractable models as the ultimate goal. In this respect, the direct certification tools developed here may help bridge the gap between the experimental certification of proof-of-principle simulations and classically intractable ones.

We thank C. Krumnow, D. Hangleiter, D. Gross, and Z. Zimboras for fruitful discussions. The work of J. E. and M. G. was funded by the Templeton Foundation, the EU (AQuS), the ERC (TAQ), and the DFG grants (SPP 1798 CoSIP, EI 519/7-1, EI 519/9-1, EI 519/14-1, and GRO 4334/2-1). The work of M. K. was funded by the National Science Centre, Poland (Polonez 2015/19/P/ST2/03001) within the European Union's Horizon 2020 research and innovation programme under the Marie Sklodowska-Curie Grant Agreement No. 665778. L. A. acknowledges financial support from the Brazilian agencies CNPq, FAPERJ, FAPESP, and CAPES.

[1] R. P. Feynman, Simulating physics with computers, Int. J. Theor. Phys. **21**, 467 (1982).
[2] J. I. Cirac and P. Zoller, Goals and opportunities in quantum simulation, Nat. Phys. **8**, 264 (2012).
[3] A. Aspuru-Guzik and P. Walther, Photonic quantum simulators, Nat. Phys. **8**, 285 (2012).
[4] R. Blatt and C. Roos, Quantum simulations with trapped ions, Nat. Phys. **8**, 277 (2012).
[5] A. A. Houck, H. E. Türeci, and J. Koch, On-chip quantum simulation with superconducting circuits, Nat. Phys. **8**, 292 (2012).

[6] I. Bloch, J. Dalibard, and S. Nascimbene, Quantum simulations with ultracold quantum gases, Nat. Phys. **8**, 267 (2012).

[7] C. Schneider, D. Porras, and T. Schaetz, Experimental quantum simulations of many-body physics with trapped ions, Rep. Prog. Phys. **75**, 024401 (2012).

[8] J. Eisert, M. Friesdorf, and C. Gogolin, Quantum many-body systems out of equilibrium, Nat. Phys. **11**, 124 (2015).

[9] A. Acin, I. Bloch, H. Buhrman, T. Calarco, C. Eichler, J. Eisert, D. Esteve, N. Gisin, S. J. Glaser, F. Jelezko, S. Kuhr, M. Lewenstein, M. F. Riedel, P. O. Schmidt, R. Thew, A. Wallraff, I. Walmsley, and F. K. Wilhelm, The European quantum technologies roadmap, arXiv:1712.03773.

[10] H. Friedenauer, H. Schmitz, J. Glueckert, D. Porras, and T. Schaetz, Simulating a quantum magnet with trapped ions, Nat. Phys. **4**, 757 (2008).

[11] K. Kim, M.-S. Chang, S. Korenblit, R. Islam, E. E. Edwards, J. K. Freericks, G.-D. Lin, L.-M. Duan, and C. Monroe, Quantum simulation of frustrated Ising spins with trapped ions, Nature (London) **465**, 590 (2010).

[12] R. Islam, E. E. Edwards, K. Kim, S. Korenblit, C. Noh, H. Carmichael, G.-D. Lin, L.-M. Duan, C.-C. J. Wang, J. K. Freericks, and C. Monroe, Onset of a quantum phase transition with a trapped ion quantum simulator, Nat. Commun. **2**, 377 (2011).

[13] B. Lanyon, C. Maier, M. Holzäpfel, T. Baumgratz, C. Hempel, P. Jurcevic, I. Dhand, A. Buyskikh, A. Daley, M. Cramer *et al.*, Efficient tomography of a quantum many-body system, Nat. Phys. **13**, 1158 (2017).

[14] R. Barends, A. Shabani, L. Lamata, J. Kelly, A. Mezzacapo, U. Las Heras, R. Babbush, A. Fowler, B. Campbell, Y. Chen *et al.*, Digitized adiabatic quantum computing with a superconducting circuit, Nature (London) **534**, 222 (2016).

[15] H. Bernien, S. Schwartz, A. Keesling, H. Levine, A. Omran, H. Pichler, S. Choi, A. S. Zibrov, M. Endres, M. Greiner, V. Vuletic, and M. D. Lukin, Probing many-body dynamics on a 51-atom quantum simulator, Nature (London) **551**, 579 (2017).

[16] Y. Salathé, M. Mondal, M. Oppliger, J. Heinsoo, P. Kurpiers, A. Potočnik, A. Mezzacapo, U. Las Heras, L. Lamata, E. Solano, S. Filipp, and A. Wallraff, Digital Quantum Simulation of Spin Models with Circuit Quantum Electrodynamics, Phys. Rev. X **5**, 021027 (2015).

[17] P. Pfeuty, The one-dimensional Ising model with a transverse field, Ann. Phys. (N.Y.) **57**, 79 (1970).

[18] S. Sachdev, Quantum phase transitions, Handbook of Magnetism and Advanced Magnetic Materials, DOI: 10.1002/9780470022184.hmm108 (2007).

[19] A. W. Kinross, M. Fu, T. J. Munsie, H. A. Dabkowska, G. M. Luke, S. Sachdev, and T. Imai, Evolution of Quantum Fluctuations Near the Quantum Critical Point of the Transverse Field Ising Chain System $CoNb_2O_6$, Phys. Rev. X **4**, 031008 (2014).

[20] P. di Francesco, P. Mathieu, and D. Sénéchal, *Conformal Field Theory* (Springer-Verlag, New York, 2012), DOI: 10.1007/978-1-4612-2256-9.

[21] A. Y. Kitaev, Unpaired Majorana fermions in quantum wires, Phys. Usp. **44**, 131 (2001).

[22] Y.-Z. You and C. Xu, Symmetry-protected topological states of interacting fermions and bosons, Phys. Rev. B **90**, 245120 (2014).

[23] H. Katsura, D. Schuricht, and M. Takahashi, Exact ground states and topological order in interacting Kitaev/Majorana chains, Phys. Rev. B **92**, 115137 (2015).

[24] F. Pollmann, E. Berg, A. M. Turner, and M. Oshikawa, Symmetry protection of topological phases in one-dimensional quantum spin systems, Phys. Rev. B **85**, 075125 (2012).

[25] U. Grimm, Spectrum of a duality-twisted Ising quantum chain, J. Phys. A **35**, L25 (2002).

[26] H. Nishimori and K. Takada, Exponential enhancement of the efficiency of quantum annealing by non-stochastic Hamiltonians, Front. ICT, DOI: 10.3389/fict.2017.00002 (2017).

[27] P. Calabrese, F. H. Essler, and M. Fagotti, Quantum quench in the transverse field Ising chain: I. Time evolution of order parameter correlators, J. Stat. Mech. (2012) P07016.

[28] P. Calabrese, F. H. Essler, and M. Fagotti, Quantum quenches in the transverse field Ising chain: II. Stationary state properties, J. Stat. Mech. (2012) P07022.

[29] P. Calabrese and J. Cardy, Entanglement entropy and quantum field theory, J. Stat. Mech. (2004) P06002.

[30] J. Dziarmaga, Dynamics of a Quantum Phase Transition: Exact Solution of the Quantum Ising Model, Phys. Rev. Lett. **95**, 245701 (2005).

[31] M. Gluza, C. Krumnow, M. Friesdorf, C. Gogolin, and J. Eisert, Equilibration via Gaussification in Fermionic Lattice Systems, Phys. Rev. Lett. **117**, 190602 (2016).

[32] U. Schneider, L. Hackermüller, J. P. Ronzheimer, S. Will, T. B. S. Braun, I. Bloch, E. Demler, S. Mandt, D. Rasch, and A. Rosch, Fermionic transport and out-of-equilibrium dynamics in a homogeneous Hubbard model with ultracold atoms, Nat. Phys. **8**, 213 (2012).

[33] E. Knill, R. Laflamme, and G. Milburn, A scheme for efficient quantum computation with linear optics, Nature (London) **409**, 46 (2001).

[34] E. Knill, Fermionic linear optics and matchgates, arXiv:quant-ph/0108033.

[35] B. M. Terhal and D. P. DiVincenzo, Classical simulation of non-interacting-fermion quantum circuits, Phys. Rev. A **65**, 032325 (2002).

[36] S. Bravyi, Lagrangian representation for fermionic linear optics, Quantum Inf. Comput. **5**, 216 (2005).

[37] A. Kitaev, Anyons in an exactly solved model and beyond, Ann. Phys. (Amsterdam) **321**, 2 (2006).

[38] F. de Melo, P. Ćwikliński, and B. M. Terhal, The power of noisy fermionic quantum computation, New J. Phys. **15**, 013015 (2013).

[39] S. Bravyi, Classical capacity of fermionic product channels, arXiv:quant-ph/0507282.

[40] A. Ferraro, S. Olivares, and M. G. A. Paris, Gaussian states in continuous variable quantum information, arXiv:quant-ph/0503237.

[41] C. Weedbrook, S. Pirandola, R. García-Patrón, N. J. Cerf, T. C. Ralph, J. H. Shapiro, and S. Lloyd, Gaussian quantum information, Rev. Mod. Phys. **84**, 621 (2012).

[42] F. Haldane, 'Luttinger liquid theory' of one-dimensional quantum fluids. I. Properties of the Luttinger model and their extension to the general 1D interacting spinless Fermi gas, J. Phys. C **14**, 2585 (1981).

[43] J. Von Delft and H. Schoeller, Bosonization for beginners—Refermionization for experts, Ann. Phys. (Berlin) **7**, 225 (1998).
[44] E. Fradkin, *Field Theories of Condensed Matter Physics* (Cambridge University Press, Cambridge, England, 2013).
[45] D. Gross, Y.-K. Liu, S. T. Flammia, S. Becker, and J. Eisert, Quantum State Tomography via Compressed Sensing, Phys. Rev. Lett. **105**, 150401 (2010).
[46] C. A. Riofrio, D. Gross, S. T. Flammia, T. Monz, D. Nigg, R. Blatt, and J. Eisert, Experimental quantum compressed sensing for a seven-qubit system, Nat. Commun. **8**, 15305 (2017).
[47] G. Tóth, W. Wieczorek, D. Gross, R. Krischek, C. Schwemmer, and H. Weinfurter, Permutationally Invariant Quantum Tomography, Phys. Rev. Lett. **105**, 250403 (2010).
[48] M. Cramer, M. B. Plenio, S. T. Flammia, R. Somma, D. Gross, S. D. Bartlett, O. Landon-Cardinal, D. Poulin, and Y.-K. Liu, Efficient quantum state tomography, Nat. Commun. **1**, 149 (2010).
[49] S. T. Flammia and Y.-K. Liu, Direct Fidelity Estimation from Few Pauli Measurements, Phys. Rev. Lett. **106**, 230501 (2011).
[50] M. P. da Silva, O. Landon-Cardinal, and D. Poulin, Practical Characterization of Quantum Devices without Tomography, Phys. Rev. Lett. **107**, 210404 (2011).
[51] S. T. Flammia, D. Gross, Y.-K. Liu, and J. Eisert, Quantum tomography via compressed sensing: Error bounds, sample complexity, and efficient estimators, New J. Phys. **14**, 095022 (2012).
[52] L. Aolita, C. Gogolin, M. Kliesch, and J. Eisert, Reliable quantum certification of photonic state preparations, Nat. Commun. **6**, 8498 (2015).
[53] A. Steffens, M. Friesdorf, T. Langen, B. Rauer, T. Schweigler, R. Hübener, J. Schmiedmayer, C. Riofrío, and J. Eisert, Towards experimental quantum-field tomography with ultracold atoms, Nat. Commun. **6**, 7663 (2015).
[54] D. Hangleiter, M. Kliesch, M. Schwarz, and J. Eisert, Direct certification of a class of quantum simulations, Quantum Sci. Technol. **2**, 015004 (2017).
[55] J. Eisert and T. J. Osborne, General Entanglement Scaling Laws from Time Evolution, Phys. Rev. Lett. **97**, 150404 (2006).
[56] G. Ramírez, J. Rodríguez-Laguna, and G. Sierra, Entanglement over the rainbow, J. Stat. Mech. (2015) P06002.
[57] V. Eisler and Z. Zimborás, Entanglement negativity in two-dimensional free lattice models, Phys. Rev. B **93**, 115148 (2016).
[58] C. V. Kraus and J. I. Cirac, Generalized Hartree-Fock theory for interacting fermions in lattices: Numerical methods, New J. Phys. **12**, 113004 (2010).
[59] See Supplemental Material at http://link.aps.org/supplemental/10.1103/PhysRevLett.120.190501 for details on methods of fermionic linear optics and proofs of properties of fidelity witnesses, which includes Refs. [17,36,52,54,60,61].
[60] M. Gluza, https://github.com/marekgluza/Fidelity_witnesses_example.
[61] M. Wimmer, Algorithm 923: Efficient numerical computation of the Pfaffian for dense and banded skew-symmetric matrices, ACM Trans. Math. Softw. **38**, 1 (2012).
[62] O. Gühne and G. Tóth, Entanglement detection, Phys. Rep. **474**, 1 (2009).
[63] F. Fröwis, M. van den Nest, and W. Dür, Certifiability criterion for large-scale quantum systems, New J. Phys. **15**, 113011 (2013).
[64] C. Gogolin, M. Kliesch, L. Aolita, and J. Eisert, Boson-sampling in the light of sample complexity, arXiv:1306.3995v2.
[65] M. B. Hastings and T. Koma, Spectral gap and exponential decay of correlations, Commun. Math. Phys. **265**, 781 (2006).
[66] P. Jordan and W. Eugene, Über das Paulische Äquivalenzverbot, Z. Phys. **47**, 631 (1928).
[67] E. Lieb, T. Schultz, and D. Mattis, Two soluble models of an antiferromagnetic chain, Ann. Phys. (N.Y.) **16**, 407 (1961).
[68] R. Blatt and C. Roos, Quantum simulations with trapped ions, Nat. Phys. **8**, 277 (2012).
[69] R. Schmied, J. H. Wesenberg, and D. Leibfried, Quantum simulation of the hexagonal Kitaev model with trapped ions, New J. Phys. **13**, 115011 (2011).
[70] M. Mielenz, H. Kalis, M. Wittemer, F. Hakelberg, R. Schmied, M. Blain, P. Maunz, D. Leibfried, U. Warring, and T. Schaetz, Freely configurable quantum simulator based on a two-dimensional array of individually trapped ions, arXiv:1512.03559.